

NMR Studies of Chloroquine–Ferriprotoporphyrin IX Complex

Angel C. de Dios,^{*,†} Robert Tycko,[‡] Lyann M. B. Ursos,^{†,§} and Paul D. Roepe^{*,†,§}

Department of Chemistry and Department of Biochemistry and Molecular Biology Georgetown University, 37th and O Streets, Washington, D.C. 20057, and Laboratory of Chemical Physics, NIDDK, National Institutes of Health, Bethesda, Maryland 20892

Received: February 4, 2003

By examining natural-abundance ^{13}C and ^{15}N solid-state nuclear magnetic resonance (NMR) spectra of acid-precipitated chloroquine–ferriprotoporphyrin IX (CQ–FPIX) aggregates, the first direct evidence is provided for CQ–FPIX complexes in the solid state, formed in a physiologic aqueous solution that mimics the environment inside the digestive vacuole of the malaria parasite. The ^{13}C spectra demonstrate a loss of signal from aromatic sites, whereas ^{15}N experiments indicate the disappearance of the signal from the N atom of the quinoline ring. These signal losses are due to the paramagnetic Fe(III) center of FPIX. In addition, contact shifts are also observed for both ^{13}C and ^{15}N spectra, suggesting the formation of a covalent complex between CQ and FPIX in the solid state.

Introduction

With the widespread emergence and continued spread of chloroquine (CQ; see Figure 1) resistance in *Plasmodium falciparum*, it is essential to understand fully the mechanism by which antimalarial drugs function. CQ and other quinoline antimalarials have complex pharmacology but are believed to act primarily by inhibiting the conversion of heme (ferriprotoporphyrin IX, FPIX) to hemozoin, which is also known as the “malaria pigment”. FPIX is a byproduct of the proteolytic degradation of hemoglobin that occurs within the malarial parasite digestive vacuole (DV). The free monomeric or dimeric heme is toxic, whereas hemozoin is innocuous to the parasite. Interactions between CQ and one or more forms of uncrystallized heme are believed to be the key to the inhibition of hemozoin formation and, hence, are the key to CQ toxicity. Therefore, detailed molecular-level data of these interactions are warranted.

Nuclear magnetic resonance (NMR) studies of aqueous solutions of CQ and FPIX have been employed to elucidate the structure of the CQ–FPIX μ oxo dimer complex.^{1–5} These previous studies examined the solution proton spectra^{1,2,5} of CQ in the presence of FPIX μ oxo dimer. Line widths and relaxation times were utilized to elucidate the distance of each proton in CQ from the paramagnetic Fe(III) center of FPIX. Carbon resonances similarly provided clues with regard to the interaction between antimalarial drugs and FPIX.^{3,4}

The CQ–FPIX complex in solution is known to be dynamic in nature. In fact, in all solution NMR measurements, what has been observed is an average picture between free and bound CQ. Samples of varying CQ:FPIX molar ratios were consequently used to extrapolate to the NMR spectrum of the CQ–FPIX complex. All the previous studies suggested the important role that π – π interactions have in the drug–heme complex. A detailed picture that has been obtained from a combination of

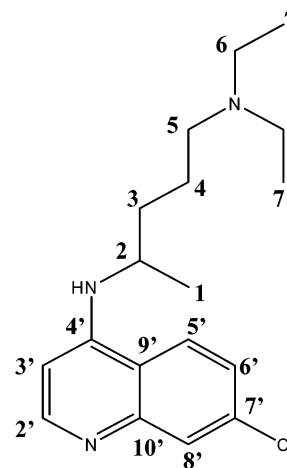


Figure 1. Schematic depiction of the 4-aminoquinoline chloroquine (CQ).

molecular dynamics simulations and longitudinal relaxation times,⁵ for instance, showed CQ atoms lying on a plane 3–5 Å above the porphyrin plane of heme. The quinoline ring lies close to the edge of the tetrapyrrole ring of heme, with both aliphatic and aromatic protons lying within the range of 3.5–6.0 Å from the Fe center. These conclusions were drawn from a quantitative analysis of the CQ proton longitudinal relaxation times in the presence of varying amounts of heme. Of course, the analysis assumed that the complex could be described by a single time-averaged structure.

The problem is not yet fully solved. The first question that comes to mind is which species of FPIX is relevant for CQ pharmacology that occurs in the DV. At pH ≥ 7 , FPIX is known to exist mainly as a μ -oxo dimer. However, in an acidic medium, FPIX can exist as a monomer. In addition, the DV, which is the subcellular organelle where both the digestion of hemoglobin and the biomineralization of FPIX to hemozoin occur, is known to be acidic.⁶ A second question arises from the dynamic nature of the complex studied in solution at neutral or alkaline pH. Because of the nonpermanent nature of the complex, it is not straightforward to discern how CQ is able to curtail hemozoin

* Authors to whom correspondence should be addressed. E-mail: dediosa@georgetown.edu, roepep@georgetown.edu.

[†] Department of Chemistry, Georgetown University.

[‡] National Institutes of Health.

[§] Department of Biochemistry and Molecular Biology, Georgetown University.

formation when the CQ–heme complex in solution is ephemeral. Lastly, solution NMR studies for these samples have been restricted to neutral or slightly alkaline solutions, because, at lower pH, heme precipitation occurs.

Therefore, the present work addresses the aggregates formed from an acidic medium that contains CQ and FPIX. These aggregates are noncrystalline solids and are, consequently, not amenable to either X-ray crystallography or solution NMR. Solid-state NMR is one technique that can still probe the nature of the interaction between CQ and FPIX in the solid state. For example, observing the ^{13}C spectra of pure CQ and the aggregate can easily provide the answer to the question of whether CQ is coprecipitating with FPIX or not. The perturbations seen in solution NMR due to the paramagnetic center are expected to be equally relevant in solid-state NMR.

Experimental Details

Ferriprotoporphyrin-IX chloride (the FPIX source) and chloroquine diphosphate (the CQ source) were purchased from Sigma (St. Louis, MO). Samples for solution NMR measurements had a starting concentration of 10 mM in CQ. Solution NMR data were collected on a Varian Unity model INOVA 500 MHz NMR spectrometer using the Varian VNMR v.5.1 software.

Ferriprotoporphyrin-IX chloride was dissolved in a pH 7.5 buffered solution to a strength of 10 mM, and equimolar CQ (from concentrated stock in the same buffer) was added. For the data shown in this paper, the solution was incubated at room temperature for 12 h; however, similar heme aggregation is observed with incubations as short as 30 min. The solution was then titrated to pH 5.0 via the addition of HCl. The addition of acid leads to the aggregation of FPIX as propionic acid side chains of the porphyrin are protonated. After a 30-min incubation at room temperature and at pH 5.0, aggregates were collected by centrifugation, lyophilized, and packed in a 3.2-mm rotor for solid-state NMR experiments. It is noteworthy that this material can be rapidly resolubilized when the acid aggregate is dissolved in alkaline solution, indicating that it is not crystalline hemozoin. Similar procedures (but without CQ added) verified that acid-aggregated FPIX alone does not produce the spectral features presented in this paper, nor does a physical mixture of FPIX and CQ powders.

^{13}C solid-state NMR measurements were acquired at a proton frequency of 400 MHz and magic-angle spinning (MAS) frequencies of 15 kHz, using a 3.2-mm rotor, a contact time of 2 ms, and a decoupling field (two-pulse phase modulation) of 100 kHz. ^{15}N spectra were obtained at a proton frequency of 600 MHz and an MAS frequency of 5 kHz. Several spectral editing techniques were employed to obtain partial resonance assignments. ^{13}C NMR spectra were externally referenced to tetramethylsilane (TMS), and ^{15}N NMR shifts were referenced to solid ammonium chloride (NH_4Cl).

Results and Discussion

Before presenting the results obtained from solid-state NMR studies, the solution ^{13}C spectra of three aqueous solutions of CQ with varying amounts of FPIX are shown in Figure 2. These spectra were obtained under typical liquid-state NMR conditions, i.e., with low proton broadband decoupling, no cross polarization, and no MAS. The signal-to-noise ratios in the spectra are different, albeit all the samples had a CQ concentration of 10 mM. The reduction in peak height is due to two reasons: (i) broadening of the resonance signals as FPIX is added, and (ii) reduction in the amount of dissolved CQ due to precipitation.

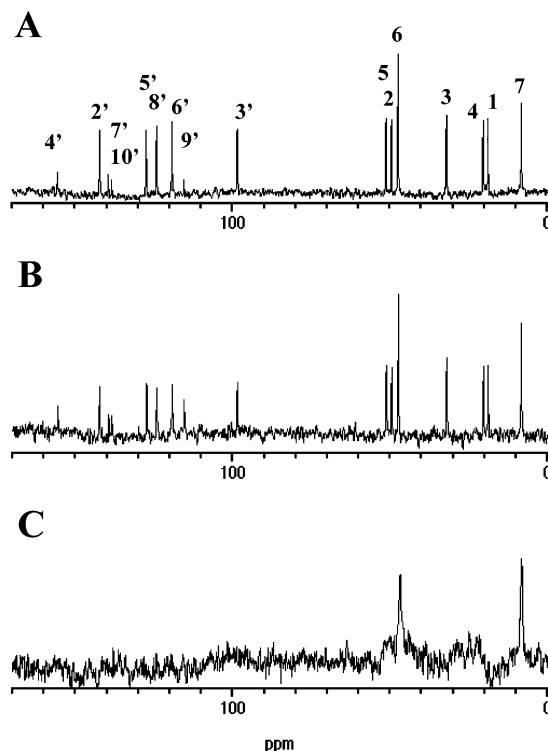


Figure 2. Proton-decoupled ^{13}C NMR spectra of solutions containing various molar ratios of CQ:FPIX: (A) CQ, no FPIX; (B) CQ:FPIX = 10:1; and (C) CQ:FPIX = 1:1. Peak labels correspond to those of Figure 1.

Even at neutral or slightly alkaline pH, aggregates are already formed with the relatively high concentrations of CQ and FPIX used in these samples. Similar to what has been observed in the proton spectrum,⁵ both aromatic and aliphatic resonances are perturbed. Also, there are no dramatic changes in the chemical shifts as the amount of FPIX increases. The solution spectrum of the 10:1 (CQ:FPIX) sample (Figure 2B) shows no movement in the position of the peaks. In addition, the 1:1 spectrum (Figure 2C) shows dramatic broadening of all the peaks. Only two signals remain easily discernible. These peaks correspond to the terminal ethyl groups of CQ. There are broad features remaining in the range of 20–30 ppm and at ~50 ppm. These regions correspond to the frequencies where the resonances of the other aliphatic C atoms are observed. Thus, in solution, the peaks become broader, but there is no noticeable change in the chemical shifts, in complete agreement with the previous proton studies.⁵

The observed chemical shifts in paramagnetic systems can be attributed to two terms:

$$\delta_{\text{observed}} = \delta_{\text{diamagnetic}} + \delta_{\text{hyperfine}} \quad (1)$$

where the diamagnetic shift corresponds to the values for the free ligand, whereas the hyperfine shift is primarily due to the presence of a paramagnetic center. Thus, if there are dramatic changes observed in the chemical shift, these can be attributed to the hyperfine shift. The hyperfine shift can be further decomposed into two contributions:^{7–11}

$$\delta_{\text{hyperfine}} = \delta_{\text{contact}} + \delta_{\text{dipolar}} \quad (2)$$

These two terms differ from each other in their mechanism. Contact shifts (δ_{contact}) are caused by spin delocalization of the unpaired electrons through chemical bonds. The magnitude of these contact shifts is proportional to the Fermi contact spin

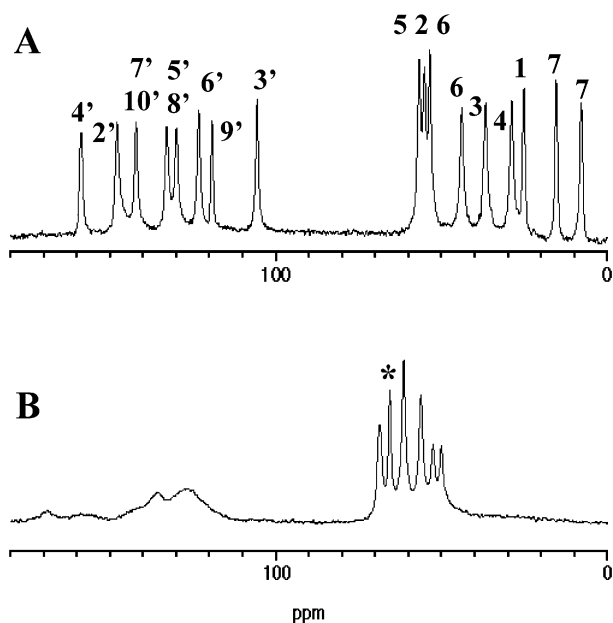


Figure 3. ^{13}C MAS NMR spectra of (A) CQ and (B) the CQ–FPIX aggregate. Peak labels correspond to those of Figure 1. The peak marked with an asterisk (*) has been assigned to the C2 atom (see text). The spectra were collected at a MAS speed of 15 kHz, a CP contact time of 2 ms, a recycle delay of 2 s, and with 65536 transients. The proton radio frequency (rf) field used for CP is 70 kHz and that for decoupling is 100 kHz.

density, which is a measure of the net imbalance between α and β spins at the site of the nucleus of interest. The spin density can either be positive or negative; therefore, it is possible to see contact shifts of opposite signs among various sites within one ligand. Dipolar shifts (δ_{contact}), on the other hand, result from a through-space interaction and are proportional to $1/r^3$, where r is the distance between the paramagnetic center and the nucleus of interest. Dipolar shifts, being dependent only on position and not chemical bonds, are expected to be independent of the identity of the nucleus.

Solution ^1H NMR studies,⁵ similar to the ^{13}C solution measurements shown in this paper, indicate no significant changes in the chemical shifts of the various protons of CQ when FPIX is introduced. Thus, in solution, as indicated by both ^1H and ^{13}C spectra, the major perturbation observed lies in the line width, and not in the position of the resonances. Furthermore, the proton spectra⁵ indicate a broadening of all signals, aliphatic and aromatic, which is an observation that, combined with a quantitative analysis of relaxation times, leads to a π – π complex picture for CQ–FPIX.

The situation in the solid state is markedly different. Figure 3 shows the spectra obtained for crystalline CQ and the aggregate of CQ–FPIX. The assignments shown are made on the basis of additional experiments that involve relaxation times, dipolar dephasing, and cross-polarization (CP) mixing times of the type described below. These parameters can help distinguish between C nuclei on the basis of the number of attached protons. Combined with the solution NMR data, each of the peaks in Figure 3A can be assigned.

There are differences between the solution and solid-state ^{13}C NMR spectra of CQ. The terminal ethyl C atoms are inequivalent in the solid-state ^{13}C NMR spectrum. To gain further insights, in regard to ^{13}C chemical shifts, ab initio calculations of the chemical shifts have been employed using Gaussian94.¹² In these calculations, an isolated CQ molecule is used. Results predict a difference of 10 ppm between the isotropic shifts of

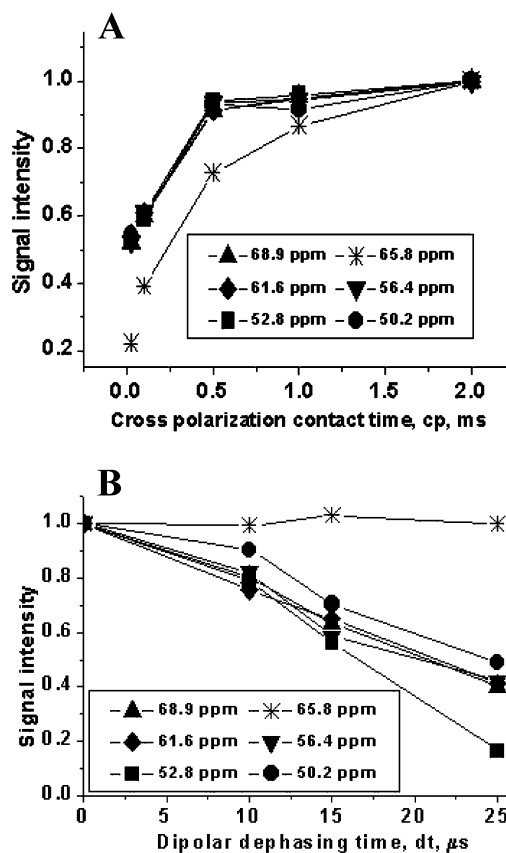


Figure 4. Results of spectral editing of the ^{13}C MAS NMR spectrum of CQ–FPIX: (A) observed signal intensity as a function of the CP contact time and (B) observed signal intensity as a function of the length of the dipolar dephasing period.

the methylene CH_2 sites (labeled as “6” in Figure 1) in the two terminal ethyl branches. These theoretical numbers are consistent with the observed shifts shown in Figure 3A. On the other hand, calculations predict a difference of only 2 ppm between the two methyl C atoms (labeled as “7” in Figure 1). Thus, the 8-ppm difference between the two C7 sites observed in the solid-state ^{13}C spectrum of CQ should be attributed to intermolecular contributions due to crystal-packing effects. Nonetheless, the assignments shown in Figure 3A are in agreement with the order provided by ab initio results.

The solid-state ^{13}C NMR spectrum of the CQ–FPIX aggregate (Figure 3B) is dramatically different from that of pure CQ in either the solution or the solid state. It is important to note that FPIX is completely invisible in this spectrum. The solid-state spectrum obtained from a rotor filled with FPIX is not different from that of an empty rotor. Consequently, the signals seen in Figure 3B arise solely from CQ. None of the NMR lines in Figure 3A appear in Figure 3B, indicating that CQ is coprecipitated with FPIX upon acidification of a 1:1 (CQ:FPIX) solution. This implies that a complex is formed between CQ and FPIX in the solid state; this complex is a potential inhibitor of hemozoin crystallization that will hinder the formation of Fe–O bonds in the tethered dimer unit cell of hemozoin.¹³

A second observation is the severe broadening of the peaks in the aromatic region. A complete assignment of the peaks in the spectrum of the aggregate is not possible at this time. However, by employing spectral editing techniques, it is possible to make partial assignments of the aliphatic peaks. Figure 4 displays the results of two experiments aimed at discriminating the six lines that are observed in Figure 3B. Data in Figure 4A

were obtained by varying the CP contact time prior to acquisition of free-induction decay (FID) signals. In this experiment, C nuclei with stronger dipole–dipole couplings to protons should exhibit a more rapid buildup of signal intensity. For instance, the signal from methylene (CH₂) C atoms should grow faster than methine (CH) C atoms. Methyl C atoms are expected to require longer mixing times, because the dipolar interactions in this case are attenuated strongly by free methyl rotation. Figure 4A therefore suggests that one of the six peaks (labeled with an asterisk (“*”) in Figure 3B, at 65.8 ppm) is not attributable to a methylene C atom, whereas the other five peaks are attributed to methylene C atoms. Data in Figure 4B were obtained by introducing a rotor-synchronized spin–echo with a short dipolar dephasing period (i.e., a period with no proton decoupling) before FID acquisition. In this experiment, signals from ¹³C nuclei with stronger couplings to protons decay more rapidly. Figure 4B clearly implies that the peak at 65.8 ppm is from a ¹³C site with relatively weak proton couplings, i.e., a rotating methyl C atom.

The signals from the quinoline C atoms have been severely broadened by the presence of the paramagnetic Fe(III) center in FPIX. There are nine C atoms on the aliphatic side chain of CQ, yet only six C atoms are observed in the aggregate. It is suggested that the missing peaks are resonances from the C2 and C7 atoms for the following reasons. As noted earlier, the methyl C7 atom seems to be especially susceptible to its environment, and in a disordered noncrystalline solid, it is reasonable to suggest that these lines have been significantly inhomogeneously broadened, that they are now buried under the baseline. Thus, the methyl C atom observed in Figure 3B is C1. In the meantime, C2, which is the aliphatic C atom lying closest to the quinoline ring, may have suffered the same fate as the quinoline C atoms.

A third observation is an apparent change in the position of the resonances, which suggests the presence of hyperfine shifts. This observation is obvious even without a complete assignment of the spectrum shown in Figure 3B. The peaks have clearly become deshielded, which is an observation that is not observed in solution (Figure 2). For example, the CQ–FPIX spectrum now has a signal at 65.8 ppm that is due to a methyl C atom, which is at least 40 ppm downfield from any of the methyl resonances observed in the spectrum of pure CQ.

To explore the nature of these hyperfine shifts further, natural-abundance ¹⁵N MAS NMR spectra of the same samples were acquired. Figure 5A displays the ¹⁵N MAS NMR spectrum of crystalline CQ. Ab initio calculations of the ¹⁵N chemical shift tensors provide the following absolute isotropic shielding (σ) and anisotropy values ($\Delta\sigma$): quinoline N ($\sigma = 113$ ppm, $\Delta\sigma = 163$ ppm), aniline-type N ($\sigma = 137$ ppm, $\Delta\sigma = 76$ ppm), and aliphatic N ($\sigma = 217$ ppm, $\Delta\sigma = 22$ ppm). The peaks shown in Figure 5A are located at 119.4, 83.2, and 16.3 ppm. On the basis of the isotropic shielding values provided by ab initio calculations, the following assignments can be made. The most deshielded peak (119.4 ppm) belongs to the N atom of the quinoline ring, whereas the most shielded peak (16.3 ppm) is attributed to the aliphatic N atom. If hyperfine shifts are expected, assignments based on ab initio calculations are no longer possible without prior knowledge of the complex structure. However, a closer inspection of the ab initio results provides an excellent parameter that can be used to discriminate between these various N sites. The shielding anisotropy obviously varies substantially from one site to the next. The quinoline N atom has a much larger anisotropy (163 ppm), whereas the aliphatic N atom is predicted to have an anisotropy of only 22

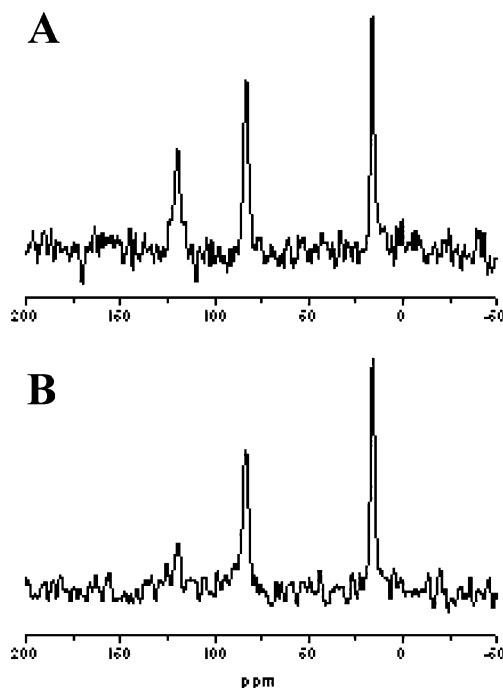


Figure 5. ¹⁵N MAS NMR spectra of CQ (A) without and (B) with CSA recoupling. The spectra were collected at a MAS speed of 5 kHz, a CP contact time of 2 ms, and a recycle delay of 2 s, with 33 000 transients. The CSA recoupling is achieved by introducing three π pulses inside two rotor periods, immediately after CP and before FID acquisition. One of these π pulses is placed at the center of the rotor period to refocus isotropic shifts. Two π pulses are then placed symmetrically with respect to the center, with the first one being applied 20 μ s after CP. The proton radio frequency (rf) field used for CP is 50 kHz and that for decoupling is 100 kHz.

ppm. The aniline-type N atom is expected to have an intermediate value for its anisotropy. It is possible to reintroduce chemical shift anisotropy (CSA) in MAS experiments by inserting three π pulses inside two rotor periods right after CP, and before acquisition of the FID.¹⁴ These three π pulses prevent refocusing of the anisotropic shifts. The intensity of the resulting signals in the CSA-recoupled experiment is anticipated to change, with the signals from sites that have larger anisotropy decreasing more substantially. Figure 5B demonstrates the discriminating ability of CSA recoupling. In agreement with the assignments suggested by the ab initio calculations, it is apparent that the most deshielded peak (assigned to the quinoline N atom) decreased the most. This peak, at 119.4 ppm, loses 65% of its signal intensity upon CSA recoupling, whereas the resonance at 83.2 ppm decreases by 34%. The most shielded resonance, which is attributed to the aliphatic N atom, changes the least ($\sim 20\%$).

The ¹⁵N MAS spectrum of the CQ–FPIX aggregate is shown in Figure 6A. Similar to the ¹³C results, the spectrum of CQ is perturbed significantly upon the addition of FPIX. First, only two resonances are observed. Second, there is a dramatic change in the isotropic shifts for the two signals observed. With CSA recoupling, it becomes evident that the two resonances can be assigned to the aliphatic N atom (-8.0 ppm), because this signal does not change appreciably with CSA recoupling, and the aniline-type N atom (11.3 ppm), which shows a decrease in intensity of $\sim 36\%$ upon CSA recoupling. The quinoline N atom is missing in the CQ–FPIX spectrum. Comparing the ¹⁵N spectrum of the aggregate to that of pure CQ establishes an upfield shift, opposite to the downfield shift seen in the ¹³C

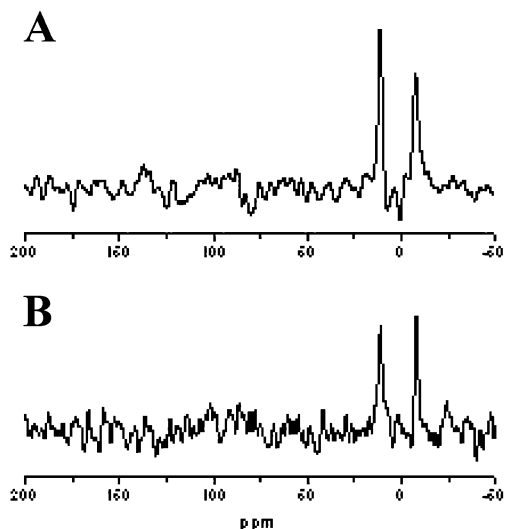


Figure 6. ^{15}N MAS NMR spectra of CQ–FPIX (A) without and (B) with CSA recoupling. These spectra are obtained under the same conditions as in Figure 5, but with 80 000 transients.

spectra. This observation is also independent of the peak assignments.

The N sites belong to the same aliphatic side chain that contains the C sites; therefore, this observation of hyperfine shifts of opposing signs points to the presence of contact shifts. Contact shifts suggest the delocalization of the unpaired electrons on the Fe(III) center through chemical bonds. A covalent complex is therefore formed between FPIX and CQ in the solid state. For the unpaired electrons on the Fe(III) center to be delocalized into the bonds in CQ, there should be a covalent bond between the Fe(III) center and one of the atoms on the quinoline ring of CQ. Our data suggest that a covalent complex between CQ and FPIX is formed in the solid state by a bond between the Fe(III) center of FPIX and the quinolinic N atom of CQ.

Conclusions

Based on ^{13}C and ^{15}N solid-state NMR experiments, it has been shown that chloroquine (CQ) coprecipitates with ferriprotoporphyrin IX (FPIX) upon acidification of a CQ–FPIX solution. The presence of contact shifts and a dramatic perturbation in the spectra of CQ demonstrates that a covalent complex between CQ and FPIX is formed in the aggregate. A covalent CQ–FPIX complex in an acid-precipitated state could act as a hemozoin crystallization poison by preventing Fe–O bonds in the tethered dimer unit cell.¹³ A fully developed digestive vacuole is acidic;⁶ however, a less-mature parasite likely harbors less-acidic (immature) vacuoles. Thus, depending on when CQ is administered, relative to the stage of parasite development,

this covalent complex might have variable toxic effects that parallel the well-known stage-specific potency of CQ. Spontaneous formation of this complex in acid aqueous solution significantly modifies our knowledge of antimalarial pharmacology and our appreciation of possible molecular pathways to CQ resistance. Additional studies that focus on the kinetics, pH, and salt dependencies of this reaction will be informative. Future solid-state NMR studies with site-specific ^{13}C and ^{15}N labeling will define the geometry of the complex.

Acknowledgment. We thank Drs. J. C. C. Chan, A. T. Petkova, and N. A. Oyler for help with NMR spectra, and Dr. A. Kosar and Ms. S. W. Hamilton for additional help. This work was supported in part by a CAREER Award from the National Science Foundation (under Grant No. CHE-9874424). Acknowledgment is made to the donors of the Petroleum Research Fund (No. 33906-AC4), administered by the American Chemical Society, the United States Public Health Service, National Institutes of Health, and the Burroughs Wellcome Fund for partial support of this research.

References and Notes

- (1) Moreau, S.; Perly, B.; Biguet, J. *Biochimie* **1982**, *64*, 1015.
- (2) Moreau, S.; Perly, B.; Chachaty, C.; Deleuze, C. *Biochim. Biophys. Acta* **1985**, *840*, 107.
- (3) Constantinidis, I.; Satterlee, J. D. *J. Am. Chem. Soc.* **1988**, *110*, 927.
- (4) Constantinidis, I.; Satterlee, J. D. *J. Am. Chem. Soc.* **1988**, *110*, 4391.
- (5) Leed, A.; DuBay, K.; Ursos, L. M. B.; Sears, D.; de Dios, A. C.; Roepe, P. D. *Biochemistry* **2002**, *41*, 10245.
- (6) Dzekunov, S. M.; Ursos, L. M. B.; Roepe, P. D. *Mol. Biochem. Parasitol.* **2000**, *110*, 107.
- (7) Walker, F. A. In *The Porphyrin Handbook*; Kadish, K. M., Smith, K. M., Guilard, R., Eds.; Academic Press: San Diego, CA, 2000; Vol. 5, pp 81–184.
- (8) Jesson, J. P. In *NMR of Paramagnetic Molecules: Principles and Applications*; La Mar, G. N., Horrocks, W. D., Jr., Holm, R. H., Eds.; Academic Press: New York, 1973; pp 1–52.
- (9) La Mar, G. N. In *NMR of Paramagnetic Molecules: Principles and Applications*; La Mar, G. N., Horrocks, W. D., Jr., Holm, R. H., Eds.; Academic Press: New York, 1973; pp 86–127.
- (10) Bertini, I.; Luchinat, C. *NMR of Paramagnetic Substances*; Coordination Chemistry Reviews 150; Elsevier: Amsterdam, 1996; pp 1–300.
- (11) Mao, J.; Zhang, Y.; Oldfield, E. *J. Am. Chem. Soc.* **2002**, *124*, 13911.
- (12) Frisch, M. J.; Trucks, G. W.; Schlegel, H. B.; Gill, P. M. W.; Johnson, B. G.; Robb, M. A.; Cheeseman, J. R.; Keith, T.; Petersson, G. A.; Montgomery, J. A.; Raghavachari, K.; Al-Laham, M. A.; Zakrzewski, V. G.; Ortiz, J. V.; Foresman, J. B.; Cioslowski, J.; Stefanov, B. B.; Nanayakkara, A.; Challacombe, M.; Peng, C. Y.; Ayala, P. Y.; Chen, W.; Wong, M. W.; Andres, J. L.; Replogle, E. S.; Gomperts, R.; Martin, R. L.; Fox, D. J.; Binkley, J. S.; Defrees, D. J.; Baker, J.; Stewart, J. P.; Head-Gordon, M.; Gonzalez, C.; Pople, J. A. *Gaussian 94*, revision C.2; Gaussian, Inc.: Pittsburgh, PA, 1995.
- (13) Pagola, S.; Stephens, P. W.; Bohle, D. S.; Kosar, A. D.; Madsen, S. K. *Nature* **2000**, *404*, 307.
- (14) Blanco, F. J.; Tycko, R. *J. Magn. Reson.* **2001**, *149*, 131.